

# Receiver Metric Design for Short-Block Channels : A Perspective for Reliable 6G Signaling Scenarios

Mody Sy and Raymond Knopp   
EURECOM, 06410 BIOT, France  
mody.sy@eurecom.fr, raymond.knopp@eurecom.fr

**Abstract**—This paper introduces receiver metrics for joint estimation and detection in short block length channels, emphasizing enhanced performance for advanced receivers, especially in scenarios with unknown channel state information and low training dimension density. Utilizing a complete 5G transceiver chain for Polar and LDPC coded transmissions paired with QPSK modulation, we analyze interleaved reference signals and data over a small number of OFDM symbols, preventing near-perfect channel estimation. Suited for mini-slot transmissions in ultra-reliable, low-latency communications, our evaluation covers up to SIMO and SU-MIMO transmission configurations over Rayleigh block fading and Line-Of-Sight channels. Results show that, with detection windows of about four modulated symbols, the proposed BICM metrics achieve detection performance that is close to that of a coherent receiver with perfect channel state information for both polar and LDPC coded configurations.

**Index Terms**—Coded Modulation metrics, 5G NR Polar code, 5G NR LDPC code, Unknown Channel State Information, Joint Estimation and Detection.

## I. INTRODUCTION

The 6G air interface is expected to build on the ideas established by the 5G standard, stressing novel paradigms in receiver algorithm design for short data transmission. Although 5G transmission formats enable very short-packet transmission through mini-slots, the ratio of training information to data may not be optimally configured for extremely brief data transmission. Additionally, the existing transmission formats are tailored for traditional quasi-coherent receivers, which may prove suboptimal in scenarios where accurate channel estimation is unattainable due to sporadic transmission of short packets. This challenge is particularly evident in cases with stringent decoding latency constraints, such as those arising in *ultra-reliable-low-latency communication* (URLLC) industrial IoT applications. The salience of advanced receiver design is particularly pronounced in scenarios characterized by error-prone communication channels, demanding a heightened level of reliability. Its efficacy depends on detection and decoding metrics, requiring a delicate balance between enhanced performance and low complexity.

Furthermore, there is a wealth of literature on *bit-interleaved coded modulation* (BICM) receivers from various perspectives demonstrating their potential impact and importance in wireless communication. We express a specific interest in BICM *multiple-input multiple-output* (MIMO) receivers, underscoring a focused inquiry into this area. In the early 21st century, noteworthy advancements were put forth in the design of maximum likelihood receivers tailored for MIMO systems [1]–[3]. Afterwards, numerous research inquiries have been directed towards the design of low-complexity receivers for

BICM MIMO, with a particular focus on low-dimensional and high-dimensional MIMO systems, but primarily restricted to coherent communication. More recently, particular attention has been paid to machine-learning-based MIMO receiver designs [4], [5]. Upon revisiting the core of this investigation, namely the transmission of short packets, it becomes apparent that this area has attracted noteworthy scholarly interest in recent years. Considerable research efforts have been dedicated to various facets, including the design of signal codes [6], enhanced receiver algorithms [7]–[12], as well as establishing state-of-the-art converse and achievability bounds for coherent and non-coherent communications [13]–[15].

This work stands out from prior literature by introducing a novel BICM receiver design within the imperfect *channel state information* (CSI) scenario, aiming to assess the impact of various channel conditions. Hence, we present enhanced receiver metrics for short data in the range of 20–100 bits for the envisaged beyond 5G/6G signaling scenarios by evaluating their performance over 5G short block channels, utilizing polar and *low-density parity-check* (LDPC) coded formats. We look into receiver metrics exploiting *joint estimation and detection* (JED) which is amenable to situations where low-density *demodulation reference signals* (DMRS) are interleaved with coded data symbols. We specifically address situations where accurate channel estimation is impossible, demonstrating that a well-conceived metric exploiting interleaved DMRS in the detection metric computation achieves performance comparable to a receiver with perfect channel state information. Remarkably, this approach demonstrates substantial performance gains when compared to conventional 5G *orthogonal frequency division multiplexing* (OFDM) receivers applicable to both uplink and downlink transmission scenarios. The proposed scheme performs detection over contiguous groups of modulated symbols including those from the DMRS to provide soft metrics for the bits in each set to the channel decoder. Explicitly, our main proposal consists in the non-coherent metric design/use in which channel estimation based on averaging/smoothing over the number of dimensions exhibiting channel coherence, constitutes a part of the metric for generating the *log likelihood ratio* (LLR) outputs.

Our contributions span the following principal avenues. Initially, we introduce BICM receiver metrics to accommodate the challenges posed by block fading channels, particularly within a  $(N_R \times N_T)$  *single-user* MIMO system. In the second phase, we proposed BICM metrics designed for a  $(N_R \times 2)$  SU-MIMO configuration, specifically tailored for line-of-sight channels. Lastly, we employ a new joint estimation

and detection approach suitable for the proposed innovative receiver architectures, resulting in a notable enhancement in overall performance.

The article is structured as follows. Section II presents the system model, and foundations of 5G polar and 5G LDPC coded modulations. Section III highlights the proposed receiver metrics, Section IV presents results and performance analysis, and Section V concludes the paper.

*Notation :* Scalars are denoted by italic letters, vectors and matrices are denoted by bold-face lower-case and upper-case letters, respectively. For a complex-valued vector  $\mathbf{x}$ ,  $\|\mathbf{x}\|$  denotes its Euclidean norm,  $|\cdot|$  denotes the absolute value.  $\angle$  denotes the angle value.  $\|\cdot\|_F$  is the Frobenius norm of matrix.  $\text{tr}\{\cdot\}$  denotes the trace of matrix.  $\mathbb{E}\{\cdot\}$  denotes the statistical expectation.  $\text{Re}(\cdot)$  denotes the real part of a complex number.  $I_0(\cdot)$  is the zero-th order modified Bessel function of the first kind.  $\mathbf{I}$  is an identity matrix with appropriate dimensions.  $\mathbf{x} \in \chi_b^j = \{\mathbf{x} : e_j = b\}$  is the subset of symbols  $\{\mathbf{x}\}$  for which the  $j$ -th bit of the label  $e$  is equal to  $b = \{0, 1\}$ . The number of bits required to a symbol is denoted by  $m \triangleq \log_2(\mathcal{M})$ . The cardinality of  $\chi$  is given by  $\mathcal{M} \triangleq |\chi|$ .  $\Lambda^j(\cdot)$  denotes log likelihood ratio, with  $j = 1, 2, \dots, m$ . The superscript  $\dagger$  denotes the complex conjugate transpose or Hermitian.

## II. SYSTEMS DESIGN AND FOUNDATIONS

### A. System Model

Consider a SU-MIMO transmission model featuring multiple antenna elements in both transmitter and receiver arrays. The system's dimensions are defined by parameters  $N_R \times N_T$ , where  $N_T$  and  $N_R$  denote the numbers of antennas in the transmitter and receiver arrays, respectively. We assume no *inter-symbol interference* (ISI) and consider a time-invariant configuration, making it feasible to use the standard base-band complex-valued representation. Let  $h_{i,j}$  represent the complex-valued path gain, serving as the fading coefficient from transmit antenna  $j$  to receive antenna  $i$ . At any given time instance when the complex-valued signals  $\{\mathbf{x}_1, \mathbf{x}_2, \dots, \mathbf{x}_{N_T}\}$  are transmitted through the  $N_T$  respective antennas. The received signal  $\mathbf{y}$  belongs to the complex vector space  $\mathbb{C}^{1 \times N_T}$  while the received signal  $\mathbf{y}$  belongs to the complex vector space  $\mathbb{C}^{1 \times N_R}$ . The additive white Gaussian noise  $\mathbf{z}$  belongs to the complex vector space  $\mathbb{C}^{1 \times N_R}$  with independent real and imaginary components, each having a variance of  $\sigma^2$  in every dimension, and the channel matrix is denoted by  $\mathbf{H} \in \mathbb{C}^{N_R \times N_T}$ . The MIMO channel model is succinctly expressed as

$$\mathbf{y} = \mathbf{x}\mathbf{H} + \mathbf{z}. \quad (1)$$

However, the system model described in (1), which represents transmission within a single symbol interval, can be extended to accommodate the transmission of several consecutive vectors  $\{\mathbf{x}_1, \mathbf{x}_2, \dots, \mathbf{x}_N\}$  over the channel. Here,  $N$  denotes the total number of symbol intervals utilized for transmission. For the sake of clarity, we employ a matrix framework. As a result, we organize the transmitted, received, and noise vectors into matrices,  $\mathbf{X} = [\mathbf{x}_1, \mathbf{x}_2, \dots, \mathbf{x}_N]^T$ ,  $\mathbf{Y} = [\mathbf{y}_1, \mathbf{y}_2, \dots, \mathbf{y}_N]^T$ ,  $\mathbf{Z} = [\mathbf{z}_1, \mathbf{z}_2, \dots, \mathbf{z}_N]^T$ , respectively. The elements within the matrix  $\mathbf{H}$  represent the complex-valued channel gains between each transmit and receive antenna.

Phrased directly, the transmitted signal  $\mathbf{x}_j$  typically consists of data-dependent  $\mathbf{x}_j^{(d)}$  and data-independent  $\mathbf{x}_j^{(p)}$  components known as pilot or reference signals. The reference signals are used to mitigate channel ambiguity in time, frequency, and space. Specifically, they are employed to estimate the channel matrix  $\mathbf{H}$ . In practice, the reference signals are commonly interleaved among the data-dependent components. The number of data dimensions is denoted by  $N_d$ , and the number of reference signal dimensions is denoted by  $N_p$ , where  $N_d + N_p = N$ .

### B. Bit-Interleaved Polar/LDPC-coded Modulation

Bit-Interleaved Polar Coded Modulation is referred to as BIPCM in this paper and makes use of *CRC-aided Polar* (CA-Polar) codes, one of the basic code construction techniques established by the 3GPP Standard [16]. In addition, Bit-Interleaved LDPC Coded Modulation is referred to as BILCM. The overall representation of the BIPCM/BILCM schematic is shown in Figure 1. This figure depicts the transmit-end procedure for uplink channels over a  $(N_R \times N_T)$  point-to-point MIMO System. In both scenarios, the encoded payload undergoes rate-matching and code block concatenation prior to being fed to a QPSK modulator. This process yields a set of complex-valued modulation symbols. Subsequently, the resource allocation process is executed, wherein one or multiple OFDM symbols are utilized to allocate the modulated symbols to resource blocks and insert the DMRS resources. As illustrated in Figure 1, the resource mapping here is embedded in the same spirit as in a 3GPP *physical uplink control channel* (PUCCH) format 2 transmission [17].

It is pertinent to highlight that MIMO systems must consider how pilot symbols are spread out in the spatial dimension, in addition to the time and/or frequency dimensions. Specifically, training symbol transmission must be carried out in such a way that interference is prevented, thus ensuring accurate channel estimation. The most straightforward fashion for interleaving pilot symbols and data is arguably through time and/or frequency insertion, although other approaches such as superposition or code-division multiplexing are also possible [18]. In addition, for a block fading instance, at least  $N_T$  pilot symbols must be inserted into each coherence block, one per antenna, with  $N_p \geq N_T$  pilot symbols per coherence block [19]. Furthermore, frequency orthogonality seems to have more merit and is particularly well suited to OFDM-type systems.

### C. Perfect Channel State Information

The channel matrix  $\mathbf{H}$  is assumed to be perfectly known at the receiver. The likelihood function or conditional probability density is approximately given by:

$$p(\mathbf{Y}|\mathbf{X}, \mathbf{H}) \propto \exp\left(\frac{2}{N_0} \text{Re}(\text{tr}\{\mathbf{Y}\mathbf{H}^\dagger\mathbf{X}^\dagger\}) - \frac{1}{N_0} \|\mathbf{X}\mathbf{H}\|_F^2\right). \quad (2)$$

The LLR bit metric for the  $j$ -th bit in BICM receiver by taking the corresponding max-log approximation (i.e.,  $\log \sum_i \exp(-\lambda_i) \approx -\min(\lambda_i)$ ) of metric is shown to be

$$\begin{aligned} \Lambda^j(\mathbf{Y}) &= \max_{\mathbf{X} \in \chi_0^j} \frac{1}{N_0} \left( 2 \text{Re}(\text{tr}\{\mathbf{Y}\mathbf{H}^\dagger\mathbf{X}^\dagger\}) - \|\mathbf{X}\mathbf{H}\|_F^2 \right) \\ &\quad - \max_{\mathbf{X} \in \chi_1^j} \frac{1}{N_0} \left( 2 \text{Re}(\text{tr}\{\mathbf{Y}\mathbf{H}^\dagger\mathbf{X}^\dagger\}) - \|\mathbf{X}\mathbf{H}\|_F^2 \right). \end{aligned} \quad (3)$$

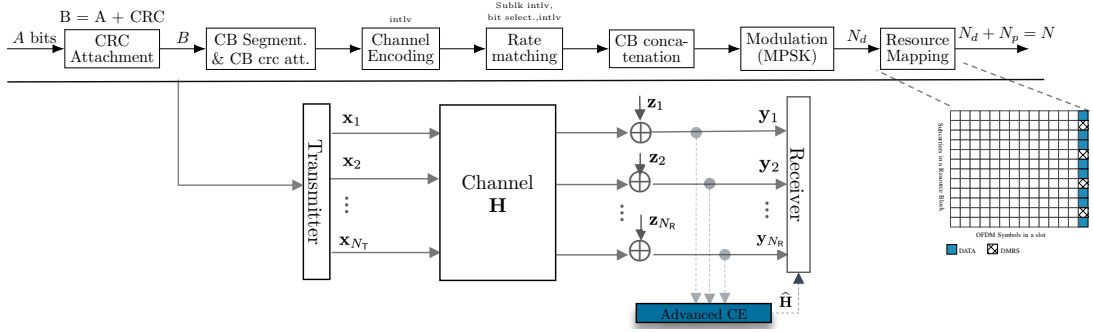


Fig. 1. Polar/LDPC coded Modulation :  $(N_R \times N_T)$  SU-MIMO System.

We consider the ideal receiver, denoted as *Perfect CSI* to be a benchmark for comparison with the subsequent receiver architectures. These subsequent architectures typically employ a separate least-squares channel estimation method by substituting the true channel matrix, denoted as  $\mathbf{H}$ , with an estimated channel matrix  $\hat{\mathbf{H}}$ . Moreover, within the framework of a conventional receiver, it is considered that, at the very least, the observation of a single reference signal spans the entirety of a *physical resource block* (PRB) or coherence block to generate the coded bit corresponding to each data symbol within that PRB. Consequently, a block is construed as comprising a singular data symbol. We will note this case throughout this paper as *No CSI* ( $N_d = 1$ ).

### III. BICM RECEIVER DESIGN WITH UNKNOWN CSI

#### A. $(N_R \times N_T)$ MIMO Rayleigh Block Fading Channel

As described earlier, the block fading channel  $\mathbf{H}$  is assumed to be a complex-valued random unitary matrix, i.e.,  $\mathbf{H} \sim \mathbb{C}\mathcal{N}(0, \mathbf{I})$ . The complex-valued fading coefficient  $h_{i,j}$  represents the channel gain between the  $j$ -th transmit antenna and the  $i$ -th receive antenna. These fading coefficients are assumed to be constant over the  $N$  symbol periods and are independent. Therefore, the probability density function of  $h_{i,j}$  can be expressed as  $p(h_{i,j}) = \frac{1}{\pi} \exp(-|h_{i,j}|^2)$ .

Both the fading coefficients and the noise follow complex Gaussian distributions. Thus, conditioned on the transmitted signal, the received signals are jointly complex Gaussian. The received signal is zero mean ( $\mathbb{E}\{\mathbf{Y}|\mathbf{X}\} = 0$ ), circularly symmetric complex Gaussian with an  $N \times N$  covariance matrix  $\Phi_Y$ , concretely.

The likelihood function or conditional probability density is commonly encountered in the literature [1], [2] and it's shown to be

$$p(\mathbf{Y}|\mathbf{X}) = \frac{\exp(-\text{tr}\{\mathbf{Y}\Phi_Y^{-1}\mathbf{Y}^\dagger\})}{\pi^{N \times N_R} \det^{N_R}(\Phi_Y)}. \quad (4)$$

It is worth noting that not all of the metric derivation steps are provided herein. Stated directly, the likelihood function can be given as :

$$p(\mathbf{Y}|\mathbf{X}) = \frac{1}{\mathbf{L}_X} \exp(-\text{tr}\{\mathbf{Y}^\dagger(N_0^{-1}\mathbf{I} - N_0^{-1}\mathbf{X}\mathbf{D}\mathbf{X}^\dagger)\mathbf{Y}\}), \text{ where } \quad (5)$$

$$\mathbf{L}_X = \pi^{N \times N_R} \det^{N_R}(N_0\mathbf{I} + \{\mathbf{X}\mathbf{X}^\dagger\}), \quad \Phi_Y^{-1} = (N_0^{-1}\mathbf{I} - N_0^{-1}\mathbf{X}\mathbf{D}\mathbf{X}^\dagger)$$

and  $\mathbf{D} = [N_0\mathbf{I} + \mathbf{X}^\dagger\mathbf{X}]^{-1}$ . This proposed likelihood function  $p(\mathbf{Y}|\mathbf{X}) = q(\mathbf{X}, \mathbf{Y})$ , commonly is referred to as the symbol

decoding metric. Ignoring the multiplicative terms independent of  $\mathbf{X}$ , (5) reduces to :

$$q(\mathbf{X}, \mathbf{Y}) \approx \frac{1}{\mathbf{L}_X} \exp\left(\frac{1}{N_0} \text{tr}\{(\mathbf{X}^\dagger\mathbf{Y})^\dagger \mathbf{D} (\mathbf{X}^\dagger\mathbf{Y})\}\right). \quad (6)$$

Observing the structure of the metrics and the absence of overlap between the data and DMRS symbols, and as shown before, we can easily see that the channel estimate is part of the metrics. By writing  $\mathbf{X} = \mathbf{X}^{(d)} + \mathbf{X}^{(p)}$ . Then, we can reveal the channel estimate  $\hat{\mathbf{H}}^{LS}$  into the metric to take full merit of the joint estimation detection principle :

$$\mathbf{X}^\dagger\mathbf{Y} = \underbrace{\mathbf{X}^{(p)\dagger}\mathbf{Y}^{(p)}}_{\text{channel estimate}} + \mathbf{X}^{(d)\dagger}\mathbf{Y}^{(d)} = \mathbf{C}_p \hat{\mathbf{H}}^{LS} + \mathbf{X}^{(d)\dagger}\mathbf{Y}^{(d)}, \quad (7)$$

where  $\mathbf{C}_p = \mathbf{X}^{(p)\dagger}\mathbf{X}^{(p)}$  given that  $\hat{\mathbf{H}}^{LS} = \frac{\mathbf{X}^{(p)\dagger}\mathbf{Y}^{(p)}}{\mathbf{X}^{(p)\dagger}\mathbf{X}^{(p)}}$ . This channel estimate is obtained via a joint *least-squares* (LS) channel estimation using averaging or smoothing over the number of dimensions exhibiting channel coherence. Note that reference signal power is typically normalized to unity. In general, the channel estimation procedure will work as usual and the resulting channel estimates are fed into the metrics considered here.

In addition, for the case of polar or LDPC-coded data, we are motivated for complexity reasons to segment the coded streams into small blocks for detection. Under an ideal interleaving assumption with known channels, detection can be performed individual modulated symbols. With joint estimation-detection and interleaved DMRS and data symbols, we will consider short blocks comprising both data and DMRS over which to compute the proposed metrics. Figure 2 shows a conceptual illustration of the proposed approach for joint estimation and detection. Consistent with this proposition, the introduced

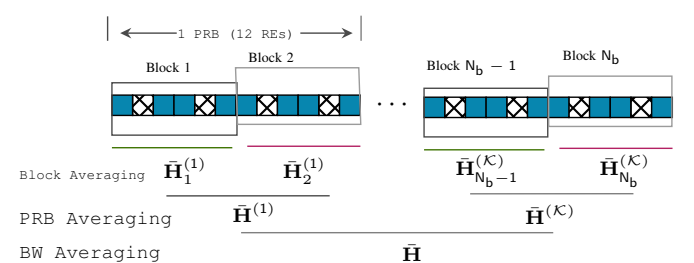


Fig. 2. Conceptual illustration of JED principle with detection windows of order  $N_d = 4$ .

---


$$\begin{aligned}\Lambda^j(\mathbf{Y}) = & \max_{\mathbf{x} \in \chi_0^j} \left( \frac{1}{N_0} \text{tr} \left\{ \left( \mathbf{C}_p \widehat{\mathbf{H}}_{LS} + \mathbf{X}^{(d)\dagger} \mathbf{Y}^{(d)} \right)^\dagger \mathbf{D} \left( \mathbf{C}_p \widehat{\mathbf{H}}_{LS} + \mathbf{X}^{(d)\dagger} \mathbf{Y}^{(d)} \right) \right\} \right) - \sum_{\mathbf{x} \in \chi_0^j} \log(\mathbf{L}_{\mathbf{x}}) \\ & - \max_{\mathbf{x} \in \chi_1^j} \left( \frac{1}{N_0} \text{tr} \left\{ \left( \mathbf{C}_p \widehat{\mathbf{H}}_{LS} + \mathbf{X}^{(d)\dagger} \mathbf{Y}^{(d)} \right)^\dagger \mathbf{D} \left( \mathbf{C}_p \widehat{\mathbf{H}}_{LS} + \mathbf{X}^{(d)\dagger} \mathbf{Y}^{(d)} \right) \right\} \right) + \sum_{\mathbf{x} \in \chi_1^j} \log(\mathbf{L}_{\mathbf{x}}).\end{aligned}\quad (11)$$


---

likelihood function enables advanced JED.

Consequently, it can be formulated as follows

$$q(\mathbf{X}, \mathbf{Y}) = \frac{1}{\mathbf{L}_{\mathbf{X}}} \exp \left( \frac{1}{N_0} \text{tr} \left\{ \left( \mathbf{C}_p \widehat{\mathbf{H}}_{LS} + \mathbf{X}^{(d)\dagger} \mathbf{Y}^{(d)} \right)^\dagger \mathbf{D} \left( \mathbf{C}_p \widehat{\mathbf{H}}_{LS} + \mathbf{X}^{(d)\dagger} \mathbf{Y}^{(d)} \right) \right\} \right). \quad (8)$$

Then, the likelihood of the coded bit  $e_j$  s.t  $b \in \{0, 1\}$  is

$$q(e_j(\mathbf{X}) = b, \mathbf{Y}) = \sum_{\mathbf{x} \in \chi_b^j} q(\mathbf{X}, \mathbf{Y}). \quad (9)$$

The LLR bit metric for the  $j$ -th bit in BICM receiver is

$$\Lambda^j(\mathbf{Y}) = \log \frac{q(e_j(\mathbf{X}) = 0, \mathbf{Y})}{q(e_j(\mathbf{X}) = 1, \mathbf{Y})}. \quad (10)$$

It is worth noting that, in the above expressions we do not limit the dimensionality of the observations when computing likelihoods of particular bits as we stated in [7]. In the original work of Caire *et al.* [20], the authors assume an ideal interleaving model which allows limiting the observation interval of a particular coded bit to the symbol in which it is conveyed. For long blocks this assumption is realistic for arbitrary modulation signal sets and is sufficient for BPSK and QPSK irrespective of the block length when the channel is known perfectly.

To ease the process of implementing such a LLR bit metric in (10), one may use its *max-log approximation* version given in (11).

Furthermore, the computational complexity of the LLR metric in a BICM MIMO system is typically on the order of  $\mathcal{O}(N_T \times N_R \times N_d \times \log_2 \mathcal{M})$ . This complexity exhibits linearity with respect to the length of received data symbols ( $N_d$ ), the number of transmitting ( $N_T$ ), and receiving ( $N_R$ ) antennas, as well as the size of the modulation alphabet ( $\mathcal{M}$ ). Considering  $N_T = 1$ , we revert to the SIMO scenario, which is similar to the proposed metric in [7] for the general non-coherent fading channel by setting the relative magnitude of the LOS component  $\alpha = 0$ , which brings the metric back to the pure Rayleigh fading case.

### B. ( $N_R \times 2$ ) MIMO Line-Of-Sight Channel

For the sake of simplicity, we consider an  $(N_R \times 2)$  MIMO configuration, acknowledging the complexity inherent in deriving metrics for spatial dimensions  $N_T > 2$  under line-of-sight channel conditions with unknown phases.

In a LOS channel represented by  $\mathbf{H}$ , covering coherence blocks of  $N$  symbols and assuming no antenna correlation, the relationship between receiver and transmitter is such that:

$$\mathbf{y}_i = \mathbf{h}_{i,1} \mathbf{x}_1 + \mathbf{h}_{i,2} \mathbf{x}_2 + \mathbf{z}_i, \quad i = 1, 2, \dots, N_R, \quad (12)$$

where  $\mathbf{y}_i \sim \mathbb{C}^{N \times i}$ ,  $\{\mathbf{x}_1, \mathbf{x}_2\} \sim \mathbb{C}^{N \times 1}$  and  $\mathbf{H} \sim \mathbb{C}^{N_R \times 2}$ . The receiver signal is then modelled as

$$\mathbf{y}_i = e^{j\theta_{i,1}} \mathbf{x}_1 + e^{j\theta_{i,2}} \mathbf{x}_2 + \mathbf{z}_i, \quad i = 1, 2, \dots, N_R. \quad (13)$$

Following the same principle as in the preceding section, we may establish the conditional probability density in order to determine the BICM metric for this typical instance. It should be stressed that  $\theta_{i,1}$  and  $\theta_{i,2}$  are unknown to the receiver and are assumed to be i.i.d. uniform random variables on  $[0, 2\pi]$ . The i.i.d. assumption for  $\theta_{i,j}$  is somewhat unrealistic for a modern array receiver with accurate calibration. The phase differences would be more appropriately characterized by two random-phases, one originating from the time-delay between transmitter and receiver and the other from the angle of arrival of the incoming wave. The phase differences of individual antenna elements for a given carrier frequency could then be determined from the angle of arrival and the particular geometry of the array. To avoid assuming a particular array geometry, the i.i.d. uniform model provides a simpler and universal means to derive a receiver metric. Upon disregarding multiplicative terms that are independent of the transmitted message, the likelihood function can be formulated as follows:

$$q(\{\mathbf{x}_1, \mathbf{x}_2\}, \mathbf{y}_i) \propto \int_{\theta_{i,1}} \int_{\theta_{i,2}} \exp \left( -\frac{1}{N_0} \|\mathbf{y}_i - e^{j\theta_{i,1}} \mathbf{x}_1 - e^{j\theta_{i,2}} \mathbf{x}_2\|^2 \right) d\theta_{i,2} d\theta_{i,1}. \quad (14)$$

By expanding the  $\ell^2$ -norms term constituting the expression of the conditional density probability, saying

$\mathbf{x}_1 \mathbf{x}_2^\dagger = |\mathbf{x}_1 \mathbf{x}_2^\dagger| e^{j\angle \mathbf{x}_1 \mathbf{x}_2^\dagger}$ ,  $\mathbf{x}_1^\dagger \mathbf{y}_i = |\mathbf{x}_1^\dagger \mathbf{y}_i| e^{j\angle \mathbf{x}_1^\dagger \mathbf{y}_i}$ ,  $\mathbf{x}_2^\dagger \mathbf{y}_i = |\mathbf{x}_2^\dagger \mathbf{y}_i| e^{j\angle \mathbf{x}_2^\dagger \mathbf{y}_i}$ , and subsequently disregarding the independent terms of  $\mathbf{x}_1$  and  $\mathbf{x}_2$ , this lends to :

$$\begin{aligned}\|\cdot\|^2 \approx & \|\mathbf{x}_1\|^2 + \|\mathbf{x}_2\|^2 + 2|\mathbf{x}_1 \mathbf{x}_2^\dagger| \cos(\theta_{i,1} - \theta_{i,2} + \angle \mathbf{x}_1 \mathbf{x}_2^\dagger) \\ & - 2|\mathbf{x}_1^\dagger \mathbf{y}_i| \cos(\theta_{i,1} - \angle \mathbf{x}_1^\dagger \mathbf{y}_i) - 2|\mathbf{x}_2^\dagger \mathbf{y}_i| \cos(\theta_{i,2} - \angle \mathbf{x}_2^\dagger \mathbf{y}_i).\end{aligned}$$

For reasons of simplicity, an assumption of orthogonality between the modulated symbols  $\mathbf{x}_1$  and  $\mathbf{x}_2$  is necessary. Actually, in MIMO systems, it is practicable or desired that the modulated symbols of distinguish antennas be orthogonal to each other. Thus, assuming orthogonality between  $\mathbf{x}_1$  and  $\mathbf{x}_2$ , this means that  $\langle \mathbf{x}_1, \mathbf{x}_2 \rangle = 0$ . Therefore, we can proceed with successive integration with respect to  $\theta_{i,1}$  and  $\theta_{i,2}$  using the *Fubini's Theorem* [21].

$$q(\{\mathbf{x}_1, \mathbf{x}_2\}, \mathbf{y}_i) \propto \exp \left( -\frac{\|\mathbf{x}_1\|^2 + \|\mathbf{x}_2\|^2}{N_0} \right) \int_{\theta_{i,1}} \exp \left( \frac{2}{N_0} |\mathbf{x}_1^\dagger \mathbf{y}_i| \cos(\theta_{i,1} - \angle \mathbf{x}_1^\dagger \mathbf{y}_i) \right) \int_{\theta_{i,2}} \exp \left( \frac{2}{N_0} |\mathbf{x}_2^\dagger \mathbf{y}_i| \cos(\theta_{i,2} - \angle \mathbf{x}_2^\dagger \mathbf{y}_i) \right) d\theta_{i,2} d\theta_{i,1}.$$

---


$$\Lambda^j(\mathbf{y}) = \max_{\{\mathbf{x}_1, \mathbf{x}_2\} \in \chi_0^j} \sum_{i=0}^{N_R-1} \frac{2}{N_0} \left( \left| N_p \hat{h}_{i,1}^{\text{LS}} + \mathbf{x}_1^{(\text{d})\dagger} \mathbf{y}_i^{(\text{d})} \right| + \left| N_p \hat{h}_{i,2}^{\text{LS}} + \mathbf{x}_2^{(\text{d})\dagger} \mathbf{y}_i^{(\text{d})} \right| - \frac{\|\mathbf{x}_1\|^2 + \|\mathbf{x}_2\|^2}{2} \right) \\ - \max_{\{\mathbf{x}_1, \mathbf{x}_2\} \in \chi_1^j} \sum_{i=0}^{N_R-1} \frac{2}{N_0} \left( \left| N_p \hat{h}_{i,1}^{\text{LS}} + \mathbf{x}_1^{(\text{d})\dagger} \mathbf{y}_i^{(\text{d})} \right| + \left| N_p \hat{h}_{i,2}^{\text{LS}} + \mathbf{x}_2^{(\text{d})\dagger} \mathbf{y}_i^{(\text{d})} \right| - \frac{\|\mathbf{x}_1\|^2 + \|\mathbf{x}_2\|^2}{2} \right). \quad (16)$$


---

Knowing that  $\frac{1}{\pi} \int_{\lambda=0}^{\pi} \exp(z \cos(\lambda)) d\lambda = I_0(z)$ , the likelihood function is shown to be

$$q(\{\mathbf{x}_1, \mathbf{x}_2\}, \mathbf{y}) \propto \prod_{i=0}^{N_R-1} \exp\left(-\frac{\|\mathbf{x}_1\|^2 + \|\mathbf{x}_2\|^2}{N_0}\right) \times I_0\left(\frac{2}{N_0} |\mathbf{x}_1^\dagger \mathbf{y}_i|\right) \times I_0\left(\frac{2}{N_0} |\mathbf{x}_2^\dagger \mathbf{y}_i|\right). \quad (15)$$

The resulting bit metric computations in logarithmic domain might be computationally hard to accomplish. For simpler processing, the *max-log approximation* is commonly used. First, an exponential approximation of  $I_0(z) \sim \frac{e^z}{\sqrt{2\pi z}} \sim e^z$  is applied. Considering this approximation, the log-likelihood ratio (LLR) for the  $j$ -th coded bit is provided in (16).

Please note that in equation (16), several terms can be omitted when the magnitude of vector  $\mathbf{x}$  remains constant, as is the scenario in BPSK or QPSK modulation.

Furthermore, the computational complexity of the LLR metric in such a BICM system is typically on the order of  $\mathcal{O}(2 \times N_R \times N_d \times \log_2 M)$ . Considering  $N_T = 1$ , we revert to the SIMO scenario, which is similar to the metric we presented in [7] for the general non-coherent fading channel by setting the relative magnitude of the LOS component  $\alpha = 1$ , which is amenable to the pure LOS scenario.

#### IV. NUMERICAL RESULTS

For illustrative purposes, we consider three distinct MIMO configurations:  $(4 \times 1)$  SIMO BICM,  $(2 \times 2)$  and  $(4 \times 2)$  MIMO BICM. The ensuing figures present the performance of BIPCM/BILCM with joint estimation and detection over a Rayleigh block fading channel and Line-of-Sight (LOS) channel. The evaluation discerns performance disparities across three scenarios: *Perfect CSI*, *No CSI* ( $N_d = 4$ ), and *No CSI* ( $N_d = 1$ ). The simulations employ NR POLAR and NR LDPC coding schemes, coupled with QPSK modulation. The transmission process encompasses a transport block length of 48 bits. The resource population procedure utilizes a single OFDM symbol with 4 PRBs or 48 resource elements (32 REs for data components and 16 REs for DMRS components). The DMRS sequences occupy 4 REs per PRB. This transmission structure, where reference and data components are concurrently transmitted within common OFDM symbols, is standard in the PUCCH or *physical uplink shared channel* (PUSCH), as well as in some downlink control channels. To conduct a comprehensive comparative analysis of our findings, we have utilized finite block length bounds, including both converses and achievability results, as established in the scientific literature. For a deeper insight into the *metaconverse* (MC) and *random coding union* (RCU) bounds utilized in the above figures, we encourage interested readers to refer to the works of authors [13]–[15].

Figure 3a shows that using the joint estimation and detection (JED) approach enhances performance by 1.5 dB and 0.75

dB for polar and LDPC coded configurations in a  $(4 \times 1)$  SIMO system with Rayleigh block fading, maintaining a *block error rate* (BLER) threshold of 1%. Despite similar code rates and transmission parameters, BIPCM consistently outperforms BILCM. This is partly due to the optimization of the 3GPP polar code for short block lengths, while the 3GPP LDPC code is designed for longer transport block lengths. Additionally, we note a performance difference of around 1.25 dB between our JED-based receiver ( $N_d = 4$ ), using BIPCM, and the metaconverse bound. Interestingly, this difference reduces to only 0.5 dB when compared to the performance of the coherent receiver with *Perfect CSI*.

Additionally, the results depicted in Figure 3b, representative of a  $(2 \times 2)$  spatially multiplexed MIMO configuration, are consistent with the trends observed in Figure 3a. However, the noticeable performance enhancements are noteworthy, indicating improvements of 0.6 dB and 0.3 dB with JED-based receivers ( $N_d = 4$ ) when employing BIPCM and BILCM, respectively.

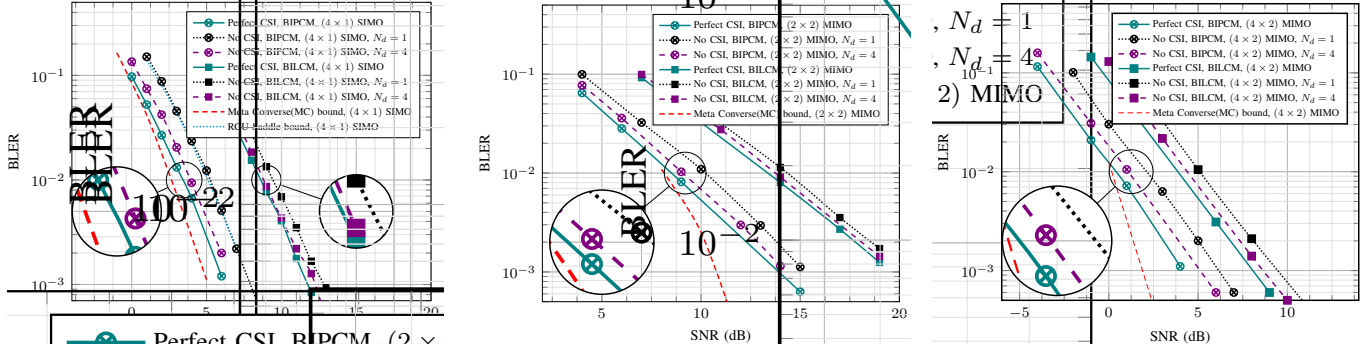
Finally, Figure 3c illustrates the  $(4 \times 2)$  BIPCM and BILCM MIMO configurations in a line-of-sight channel scenario. At a BLER of 1%, the performance comparison in the first configuration indicates a gain of 1 dB with the JED-based receiver over the conventional receiver. Additionally, there is a 0.6 dB difference between the JED-based receiver ( $N_d = 4$ ) and the *Perfect CSI* or ideal receiver. In the second configuration, specifically the  $(4 \times 2)$  BILCM MIMO, there is a 0.75 dB improvement with the JED-based receiver ( $N_d = 4$ ) compared to the conventional receiver, along with a 0.5 dB gap between the *Perfect CSI*-based receiver and the JED-based receiver ( $N_d = 4$ ).

Remarkably, it can be contended that the advanced receiver outperforms the conventional counterpart and demonstrates greater resilience in the face of inaccurate channel estimation.

Nonetheless, as delineated in a previous correspondence [7], these performance enhancements can be significantly boosted. This improvement consistently converges towards an ever-closer alignment with the performance benchmarks set by the ideal or coherent receiver, mainly through adaptive DMRS/data power adjustment as the underlying transmission forwards data and reference signals in a frequency-interleaved fashion within a common OFDM symbol. In this spirit, we can even prioritise transmission with fewer DMRS in order to *bootstrap* the advance receiver, therefore reducing some transmission overhead.

#### V. CONCLUSIONS

This paper presented receiver metrics for joint estimation and detection using training or reference signal transmission



(a)  $(4 \times 1)$  SIMO, Rayleigh Block Fading channel. (b)  $(2 \times 2)$  SU-MIMO, Rayleigh Block Fading channel. (c)  $(4 \times 2)$  SU-MIMO, Line-of-Sight (LOS) channel.  
 Fig. 3. Block Error Rate, 48 bits(TBs+CRC), NR POLAR BICM (CRC-aided successive-cancellation list decoder, List length=8), NR LDPC BICM (belief propagation decoder, iteration=30) QPSK modulation, 1 OFDM symbol, 4 PRBs, 48 REs (32 data, 16 DMRS), versus outer (MC) bound

strategies in short block length channels. We showed that it is possible to enhance the performance and sensitivity through joint detection-estimation compared to standard receivers, especially when the channel state information is unknown and the density of the training dimensions is low. The performance analysis made use of a full 5G transmitter and receiver chains for both Polar and LDPC coded transmissions paired with QPSK modulation schemes. We considered transmissions where reference signals are interleaved with data and both are transmitted over a small number of OFDM symbols so that near-perfect channel estimation cannot be achieved. We characterized the performance for up to SIMO and spatially multiplexed SU-MIMO transmission configurations in order to determine the performance gain offered by the proposed detection metrics in realistic base station receiver scenarios over Rayleigh block fading and Line-Of-Sight channels. Our findings demonstrate that when the detection windows used in the metric units is on the order of four modulated symbols the proposed receiver metrics can be used to achieve detection performance that is close to that of a coherent receiver with perfect CSI for both polar and LDPC coded configurations.

## REFERENCES

- [1] B. M. Hochwald and T. L. Marzetta, "Unitary space-time modulation for multiple-antenna communications in Rayleigh flat fading," in IEEE Transactions on Information Theory, vol. 46, no. 2, pp. 543-564, March 2000.
- [2] T. L. Marzetta and B. M. Hochwald, "Capacity of a mobile multiple-antenna communication link in Rayleigh flat fading," in IEEE Transactions on Information Theory, vol. 45, no. 1, pp. 139-157, Jan. 1999.
- [3] B. M. Hochwald and S. T. Brink, "Achieving near-capacity on a multiple-antenna channel," in IEEE Transactions on Communications, vol. 51, no. 3, pp. 389-399, March 2003.
- [4] D. F. Carrera, D. Zabala-Blanco, C. Vargas-Rosales and C. A. Azurdia-Meza, "Extreme Learning Machine-Based Receiver for Multi-User Massive MIMO Systems," in IEEE Communications Letters, vol. 25, no. 2, pp. 484-488, Feb. 2021.
- [5] S. Cammerer, F. A. Aoudia, J. Hoydis, A. Oeldemann, A. Roessler, T. Mayer and A. Keller, "A Neural Receiver for 5G NR Multi-user MIMO," ArXiv abs/2312.02601, 2023.
- [6] M. Shirvanimoghaddam et al., "Short Block-Length Codes for Ultra-Reliable Low Latency Communications," in IEEE Communications Magazine, vol. 57, no. 2, pp. 130-137, February 2019.
- [7] M. Sy, R. Knopp, "Novel Joint Estimation and Decoding Metrics for Short-Blocklength Transmission Systems," 2023 IEEE Conference on Standards for Communications and Networking (CSCN), Munich, Germany, Nov. 2023.
- [8] B. Lee, S. Park, D. J. Love, H. Ji and B. Shim, "Packet Structure and Receiver Design for Low Latency Wireless Communications With Ultra-Short Packets," in IEEE Transactions on Communications, vol. 66, no. 2, pp. 796-807, Feb. 2018.
- [9] M. Sy, R. Knopp, "Enhanced Low-Complexity Receiver Design for Short Block Transmission Systems," 34th IEEE International Symposium on Personal, Indoor and Mobile Radio Communications (PIMRC 2023), Toronto, ON, Canada, Sept. 2023.
- [10] C. Yue, V. Miloslavskaya, M. Shirvanimoghaddam, B. Vucetic and Y. Li, "Efficient Decoders for Short Block Length Codes in 6G URLLC," IEEE Communications Magazine, Vol. 61, no.4, pp 84-90, April 2023.
- [11] T. -H. Vu, T. -T. Nguyen, Q. -V. Pham, D. B. da Costa and S. Kim, "A Novel Partial Decode-and-Amplify NOMA-Inspired Relaying Protocol for Uplink Short-Packet Communications," in IEEE Wireless Communications Letters, vol. 12, no. 7, pp. 1244-1248, July 2023.
- [12] N. Doan, "Low-complexity decoding of short linear block codes with machine learning," PhD Dissertation, McGill University, May 2022.
- [13] M. Xhemrishi, M. C. Coşkun, G. Liva, J. Östman and G. Durisi, "List Decoding of Short Codes for Communication over Unknown Fading Channels," 2019 53rd Asilomar Conference on Signals, Systems, and Computers, Pacific Grove, CA, USA, 2019, pp. 810-814.
- [14] J. Östman, G. Durisi, E. G. Ström, M. C. Coşkun and G. Liva, "Short Packets Over Block-Memoryless Fading Channels: Pilot-Assisted or Noncoherent Transmission?," in IEEE Transactions on Communications, vol. 67, no. 2, pp. 1521-1536, Feb. 2019.
- [15] A. Martinez and A. G. i Fàbregas, "Saddlepoint approximation of random-coding bounds," 2011 Information Theory and Applications Workshop, La Jolla, CA, USA, 2011, pp. 1-6.
- [16] 3GPP TS 38.212 V16.2.0, "Technical Specification Group Radio Access Network, Multiplexing and channel coding", July 2020.
- [17] 3GPP TS 38.211 V16.5.0, "Technical Specification Group Radio Access Network, Physical Channels and Modulation", May 2021.
- [18] J. R. Hampton, "Introduction to MIMO Communications," Cambridge University Press, Nov. 2013.
- [19] R. W. Heath Jr., A. Lozano, "Foundations of MIMO Communication," Cambridge University Press, Dec. 2018.
- [20] G. Caire, G. Taricco and E. Biglieri, "Bit- Interleaved Coded Modulation," IEEE Transactions on Information Theory, vol. 44, pp. 927-946, May 1998.
- [21] G. Fubini, "Sugli integrali multipli", Rom. Acc. L. Rend. (5), vol. 16, no. 1, pp. 608-614, 1907.